

A parallel workflow implementation for PEST version 13.6 in high-performance computing for WRF-Hydro version 5.0: a case study over the midwestern United States

¹Jiali Wang, ¹Cheng Wang, ²Vishwas Rao, ¹Andrew Orr, ¹Eugene Yan, ¹Rao Kotamarthi

¹Argonne National Laboratory, Environmental Science Division, 9700 South Cass Avenue, Lemont, IL 60439, USA

²Argonne National Laboratory, Mathematics and Computer Science Division, 9700 South Cass Avenue, Lemont, IL 60439, USA

Correspondence to: Jiali Wang (jjaliwang@anl.gov); Rao Kotamarthi (vrkotamarthi@anl.gov)

Abstract. The Weather Research and Forecasting Hydrological (WRF-Hydro) system is a state-of-the-art numerical model that models the entire hydrological cycle based on physical principles. As with other hydrological models, WRF-Hydro parameterizes many physical processes. Hence, WRF-Hydro needs to be calibrated to optimize its output with respect to observations for the application region. When applied to a relatively large domain, both WRF-Hydro simulations and calibrations require intensive computing resources and are best performed on multimode, multicore high-performance computing (HPC) systems. Typically, each physics-based model requires a calibration process that works specifically with that model and is not transferrable to a different process or model. The parameter estimation tool (PEST) is a flexible and generic calibration tool that can be used in principle to calibrate any of these models. In its existing configuration, however, PEST is not designed to work on the current generation of massively parallel HPC clusters. To address this issue, we ported the parallel PEST to HPCs and adapted it to work with WRF-Hydro. The porting involved writing scripts to modify the workflow for different workload managers and job schedulers, as well as developing code to connect parallel PEST to WRF-Hydro. To test the operational feasibility and the computational benefits of this first-of-its-kind HPC-enabled parallel PEST, we developed a case study using a flood in the midwestern United States in 2013. Results on a problem involving calibration of 22 parameters show that on the same computing resource used for parallel WRF-Hydro, the HPC-enabled parallel PEST can speed the calibration process by a factor of up to 15 compared with commonly used

1 PEST in sequential mode. The speedup factor is expected to be greater with a larger calibration
2 problem (e.g., more parameters to be calibrated or a larger size of study area).

3 **1 Introduction**

4 Physically based hydrological models contain detailed physical mechanisms to model the
5 hydrological cycle, but many complex physical processes in these models are parameterized. For
6 example, the state-of-the-art Weather Research and Forecasting Hydrological (WRF-Hydro)
7 modeling system (Gochis et al., 2018) has dozens of parameters that can be land- and river-type
8 dependent and are typically specified in lookup tables. Therefore, these hydrological models need
9 to be calibrated before they can be applied to research over different regions. In this context,
10 calibration refers to adjusting the values of the model parameters so that the model can closely
11 match the behavior of the real system it represents. In some cases, the appropriate value for a
12 model parameter can be determined through direct measurements conducted on the real system. In
13 many situations, however, the model parameters are conceptual representations of abstract
14 watershed characteristics and must be determined through calibration. In fact, model calibration is
15 the most time-consuming step, not only for hydrological models, but also for Earth system model
16 development, because both parametric estimation and parametric uncertainty analysis require
17 hundreds—if not thousands—of model simulations to understand how perturbations in model
18 parameters affect simulations of dominant physical processes and to find the optimum value of a
19 single parameter.

20
21 WRF-Hydro is a numerical model that can simulate the entire hydrological cycle using advanced
22 high-resolution data such as satellite and radar products. Compared with the traditional land
23 surface model (LSM) used by WRF, WRF-Hydro provides a framework for multiscale
24 representation of surface flow, subsurface flow, channel routing, and baseflow, as well as a simple
25 lake/reservoir routing scheme. As a physics-based model, WRF-Hydro includes many complicated
26 physical processes that are nonlinear and must be parameterized. The default parameters given by
27 WRF-Hydro may be valid for one region but not for another region. Hence calibration of related
28 model parameters is often required in order to use the model in a new domain. In particular, for a
29 large spatial domain such as the entire contiguous United States, in order to develop the optimal
30 parameter sets in a reasonable amount of time, the calibration must be conducted on high-

1 performance computing (HPC) systems in parallel instead of in the traditional sequential mode.
2 To date, no such calibration tool can efficiently calibrate WRF-Hydro on HPC resources.
3 Typically, each physics-based model needs a calibration code that is custom designed to work with
4 that particular numerical model and its set of physics parameterizations, software architecture, and
5 solvers. These custom-designed calibration codes are highly challenging and do not offer
6 flexibility. Therefore, a more flexible and generic calibration tool is needed that can calibrate any
7 code that uses Message Passing Interface/Open Multi Processing (MPI/OpenMP) for
8 parallelization on HPC systems.

9
10 One widely used generic and independent calibration tool is the parameter estimation tool (PEST).
11 PEST (Doherty, 2016) conducts calibration automatically based on mathematical methods and
12 thus is applicable for optimizing nonlinear parameters. Compared with manual calibration,
13 automatic calibration is more efficient and effective because it avoids interference from human
14 factors (Madsen, 2000; Getirana, 2010). The uniqueness of PEST is that it operates independent
15 of models: there is no need to develop additional programs for a particular model except preparing
16 the files required by PEST (as described in Sec. 3.2). PEST has four modes of operation. One of
17 the modes is regularization mode, which supports the use of Tikhonov regularization and is found
18 better for serving environmental models because, if implemented properly, it supports model
19 predictions of minimum error variance, is numerically stable, and embraces rather than eschews
20 the heterogeneity of natural systems. Singular value decomposition (SVD) can be used as a
21 regularization device to guarantee numerical stability of the calibration problem. Parallel PEST is
22 able to distribute many runs across many computing nodes using master-worker parallel
23 programming. To our best knowledge, however, no approach is available that allows users to submit
24 jobs using PEST parallelization to a typical supercomputing facility that uses job scheduling and
25 workload management such as Simple Linux Utility for Resource Management (SLURM),
26 Portable Batch System (PBS), and Cobalt. A previous study (Senatore et al., 2015) used PEST to
27 calibrate WRF-Hydro over the Crati River Basin in southern Italy. Because the study area was
28 relatively small, the authors were able to conduct the calibration using PEST in sequential mode
29 (Alfonso Senatore, personal communication, 2018).

30

1 This study aims to (1) port parallel PEST to HPC clusters operated by the U.S. Department of
2 Energy (DOE) and adapt it to work with WRF-Hydro, (2) evaluate the performance of HPC-
3 enabled parallel PEST linked to WRF-Hydro by calibrating a flood event, and (3) explore the
4 scale-up capability and computational benefits of HPC-enabled parallel PEST by assigning
5 different computing resource to the entire calibration process.

6 **2 Model description**

7 **2.1 Study area**

8 The case presented here is one of the worst floods experienced by greater Chicago area in the past
9 three decades; the storm occurred on April 18, 2013. According to the National Weather Service
10 (NWS), the heaviest 24-hour accumulated rainfall during this storm reached 201.4, 171.1, and
11 136.4 mm across Illinois, Iowa, and Missouri, respectively. The Mississippi River crested at 10.8
12 m (1.7 m above flood stage), and the Illinois River crested in Peoria, Illinois, at 8.95 m; these river
13 cresting broke the previous record of 8.78 m, set in 1943, and was 4.55 m above the historical
14 normal river stage (NWS, 2013). Campos and Wang (2015) conducted three-domain nested WRF
15 simulations to understand the dynamical and microphysical mechanisms of the event. Our study
16 builds on the smallest domain of that study, which covers Illinois, and majority of Iowa and
17 Missouri at a spatial resolution of 3 km (Fig. 1). The domain size is $\sim 495,000 \text{ km}^2$ (747 km from
18 west to east; 657 km from south to north).

19

20 **2.2 WRF-Hydro configuration**

21 This study employs WRF-Hydro version 5 with a basic configuration. This configuration does not
22 use nudging techniques or spatially distributed soil-related parameters as used in the National
23 Water Model configuration. WRF-Hydro has been tested in several different cases that focused on
24 different hydrometeorological forecasting and simulation problems (e.g., Gochis et al., 2018;
25 Yucel et al., 2015; Senatore et al., 2015; Arnault et al., 2016), and it shows reasonable accuracy in
26 simulated streamflow after being carefully calibrated. For details of the WRF-Hydro modeling
27 system, see Gochis et al. (2018). Currently, two LSMs are available in WRF-Hydro for
28 representing land-surface column physics: Noah (Chen and Dudhia, 2001) and Noah Multi-

1 parameterization (Noah-MP; Niu et al. 2011). We utilize Noah-MP LSM because compared with
2 Noah LSM it shows obvious improvements in reproducing surface fluxes, skin temperature over
3 dry periods, snow water equivalent, snow depth, and runoff (Niu et al. 2011). The Noah-MP is
4 configured at a grid spacing of 3 km, and the aggregation factor is 15; that is, starting from a 3 km
5 LSM resolution in the domain shown in Fig. 1, hydrological routing is performed at a grid
6 resolution of 200 m, with 3285 south-north \times 3735 west-east grid cells. We use a time step of 10
7 seconds for the routing grid in order to maintain model stability and prevent numerical dispersion
8 of overland flood waves. The WRF-Hydro is configured to be in offline or uncoupled mode—there
9 is no online interaction between the WRF-Hydro hydrological model and the WRF atmospheric
10 model. Overland flow, saturated subsurface flow, gridded channel routing, and a conceptual
11 baseflow are active in this study. The gridded channel network uses an explicit, one-dimensional,
12 variable time-stepping diffusive wave. The time step of 10 seconds also meets the Courant
13 condition criteria for diffusive wave routing on a 200 m resolution grid. A direct output-equals-
14 input “pass-through” relationship is adopted to estimate the baseflow. Although the baseflow
15 module is not physically explicit, it is important because the water flow in the channel routing is
16 contributed by both the overland flow and baseflow. If the overland flow is active as it is in this
17 study, it passes water directly to the channel model. In this case the soil drainage is the only water
18 resource flowing into the baseflow buckets. However, if the overland flow is deactivated but
19 channel routing is still active, then WRF-Hydro collects excess surface infiltration water from the
20 land model and passes this water into the baseflow bucket. This bucket then contributes the water
21 from both overland and soil drainage to the channel flow. Therefore, the baseflow must be active
22 if the overland flow is switched off. This study does not consider lakes and reservoirs.

23

24 We use the geographic information system (GIS) tool (Sampson and Gochis, 2018) developed by
25 the WRF-Hydro team to delineate the stream channel network, open water (i.e., lake, reservoir,
26 and ocean) grid cells, and groundwater/baseflow basins. Meteorological input for the WRF-Hydro
27 model system includes hourly precipitation; near-surface air temperature, humidity, and wind
28 speed; incoming shortwave and longwave radiation; and surface pressure. In this study, the hourly
29 precipitation is from the National Centers for Environmental Prediction (NCEP) Stage IV analysis
30 at a spatial resolution of 4 km. The Stage IV data is based on combined radar and gauge data (Lin
31 and Mitchell, 2005; Prat and Nelson, 2015), and has been shown to be temporally well correlated

1 with high-quality measurements from individual gauges (see, e.g., Sapiano and Arkin, 2009; Prat
2 and Nelson, 2015). The other hourly meteorological inputs are from the second phase of the multi-
3 institution North American Land Data Assimilation System project, phase 2 (NLDAS-2) (Xia et
4 al., 2012a,b), at a spatial resolution of 12 km. NLDAS-2 is an offline data assimilation system
5 featuring uncoupled LSMs driven by observation-based atmospheric forcing.

6
7 During the 15-day period of this studied case, light to moderate rain occurred on April 8 through
8 11, 2013, followed by a relatively dry period from April 12 to 15. Then a heavy rain event began
9 on April 16 and peaked on April 18. The heaviest rain band moved east of the study area on April
10 19. The rainy event ended over the study area on April 20 (see Fig. S1 in Supporting Information).
11 We start the WRF-Hydro simulation on October 1, 2012, and run the model for six months to reach
12 equilibrium. This 6-month period is considered as spin-up time and is excluded from model
13 calibration and evaluation. We calibrate the river discharge calculated by the WRF-Hydro model
14 from 00UTC April 9 to 00UTC April 12, 2013, considering it long enough to achieve our objective.
15 We then evaluate the model performance against U.S. Geological Survey (USGS) observed river
16 discharge from 00UTC April 12 to 00UTC April 25, 2013.

17 **3 Calibration**

18 **3.1 Platforms**

19 We customized parallel PEST to work on three different workload managers and job schedulers:
20 SLURM at the National Energy Research Scientific Computing Center (NERSC), PBS at the
21 Argonne National Laboratory Computing Resource Center (LCRC), and Cobalt at the Argonne
22 Leadership Computing Facility. The tests presented here are conducted on Edison and Cori at
23 NERSC, and Bebop at Argonne LCRC, which all use the SLURM workload manager and job
24 scheduler.

25
26 The interface we have built between parallel PEST and the management software is, in general,
27 used for (1) setting the number of workers, and the nodes for each worker to conduct a model run
28 (WRF-Hydro here); (2) setting up the working directory for the workers; (3) finding the nodes that
29 are available; (4) identifying the nodes that work for each worker; (5) passing the global files (same

1 for all the working directory) to all the workers (these files include the lookup table files that are
2 not to be calibrated, the namelist files for both LSM and hydrological sector, and restart files that
3 generated by the previous simulations, or spin-up period); and (6) submitting the job for the entire
4 calibration process, including parallel PEST and parallel WRF-hydro. This job can be submitted
5 as a cold-start run or as a restart. The main difference for this interface on different management
6 software is that different management software has its own way to identify available nodes and to
7 submit jobs. These differences require minor changes in the scripts we developed, which involve
8 finding and identifying available nodes for workers, and submitting jobs for the specific
9 management software. See detailed comments in the published code and scripts.

10 **3.2 PEST files and settings**

11 PEST requires three file types in both sequential and parallel modes. They are template files to
12 define the parameters to be calibrated, an instruction file to define the format of model-generated
13 output files, and a control file to supply PEST with the size of the problem and the settings for the
14 calibration method. Parallel PEST uses a “master-worker” paradigm that starts model runs
15 simultaneously by different workers (or in different folders). The master of parallel PEST
16 communicates with each of its workers many times during a calibration. To run PEST in parallel
17 mode, one also needs a management file to inform PEST where the working folder is for each
18 worker and what the names and paths are for each model input file that PEST must write (i.e.,
19 lookup tables that come from template files) and each model output file that PEST must read (such
20 as frsxt_pts_out.txt). The management file also set the maximum running time for each worker.
21 For those workers that take longer than the maximum running time, PEST will stop the model run
22 by that particular worker and assign that model run to another worker if there is one with nothing
23 else to do.

24
25 To the best of our knowledge, however, parallel PEST is not designed to run on HPCs directly.
26 We developed scripts and an interface to enable parallel PEST to run on HPCs using SLURM,
27 PBS, or Cobalt workload managers and job schedulers. The development involved writing scripts
28 to modify the workflow for different workload managers and job schedulers, as well as developing
29 code to connect parallel PEST to WRF-Hydro. These developments enable parallel PEST to run
30 many workers at the same time; each worker runs a parallel code (here WRF-Hydro) that uses

1 more than one node, which could significantly reduce the wall-clock time of model calibrations.
2 Although this master-worker parallelism may not be as efficient as a fully MPI approach, it is
3 sufficient for model calibration and requires the least effort for the current parallel PEST to run on
4 HPC systems.

5
6 This study presents calibration results from PEST using the SVD-based regularization in
7 regularization mode to ensure numerical stability (Tonkin and Doherty, 2005). We focus on
8 calibrating 22 parameters (see Table 1 and detail description in Sec. 3.3) using 96 observation
9 points and 22 items of prior information for the calibrated parameters. In each item of prior
10 information, a value equal to its default value provided by the WRF-Hydro v5.0 (or the log of its
11 default value) is assigned for each adjustable parameter, assuming that default values are the
12 preferred values. All prior information equations are assigned a weight of 1.0. We assigned five
13 different regularization groups to the prior information: Manning’s roughness coefficients
14 specified by Strahler stream order in CHANPARAM.TBL to one group; the parameters in
15 HYDRO.TBL (Manning’s roughness coefficients for overland flow as a function of vegetation
16 types) to another group; and three global parameters for the Noah-MP (xslop1, refdk, and refkdt)
17 in GENPARAM.TBL to the remaining three groups. The 96 observation points are given different
18 weights based on the inversed mean of their observed discharge during the studied period (see the
19 detailed description in Sec. 3.3 and Sec. 4.1). For a detailed description of these settings see the
20 PEST User Manual (Doherty, 2016).

21

22 **3.3 Calibrated experiments**

23 The primary objective of this study is to build a bridge for linking the parallel PEST and WRF-
24 hydro on the basis of HPC clusters and to explore the computational benefits of this bridge. We
25 do not attempt to extensively assess each individual tool or address questions in each individual
26 domain, such as optimizing the objective functions in PEST or calibrating WRF-Hydro for a long
27 time period considering all the relevant parameters to achieve an optimal parameter set. The
28 calibration period thus is limited to only three days, which we believe long enough to achieve our
29 objective and to understand WRF-Hydro’s sensitivity to the calibrated parameters. We calibrated
30 WRF-Hydro using four USGS sites (referred to as Station 1, Station 2, Station 3, and Station 4

1 hereafter), as shown in Fig. 1. (More USGS sites could be included if one manually reallocated
2 the stations that were not properly assigned to the desired location on the channel network by the
3 GIS tool.) As shown by the lower left index map in Figure 1, the study area (the red box) only
4 covers the lower part of Upper Mississippi River Basin (UMRB) and a portion of Missouri River
5 Basin (MORB). In order to prepare observation datasets of streamflow contributed *only* from the
6 drainage area *within* the model domain, we identified inflows entering the model domain at three
7 different sites, namely, sites 05411500, 06807000, and 06887500, as indicated by the black solid
8 triangles in the index map of Figure 1. The outflows of combined UMRB and MORB can be found
9 at the three outlets, namely, sites 07010000, 07020500, and 07022000 (named Stations 2, 3, and
10 4, respectively, as shown by black solid circles in Figure 1). These outlets are located sequentially
11 at the main Mississippi River after confluence of Mississippi River and Missouri River. Thus, the
12 observed streamflow contributed by drainage area *within* the model domain can be calculated by
13 subtracting the sum of the discharge at the three sites (black triangles; recognized as inflow) from
14 the discharge at each of the three outlet sites (black circles; recognized as outflow). The final
15 derived observations of streamflow (or adjusted streamflow observation data) from the drainage
16 area *within* this model domain are prepared for model calibration and validation. To prove this
17 concept, we validated the consistency of the sum of observed drainage areas at inflow sites plus
18 modeled drainage area with the overall drainage area at the outlet. The drainage area (UMRB and
19 MORB) at outlet site 07010000 is $1.8E+12$ m². The sum of drainage areas at three inflow sites is
20 about $1.4E+12$ m² ($2.0E+11$, $1.1E+12$, and $1.4E+11$ m² for site 05411500, 06807000, and
21 06887500, respectively) and the modeled drainage area is $0.36E+12$ m²; the total area is $1.76E+12$
22 m². This indicates that the flows from sum of three inflow sites and modeled result represent 98%
23 of drainage area at the outflow site 07010000. Therefore, the adjusted streamflow observation data
24 are qualified for model calibration. We then transfer the calibrated parameters to other subbasins
25 in the study area to assess the transferability of the calibrated parameters. Although many
26 parameters, including spatially distributed parameters and constant parameters in the lookup
27 tables, affect the model performance, we calibrate only the parameters in lookup tables and do not
28 consider the spatial variability of other parameters or their scaling factors. We acknowledge that
29 some studies calibrate a single scaling factor (without considering its spatial variability, however)
30 of overland roughness coefficients (OVROUGHRTFAC) rather than the actual value of each land
31 type in the lookup table (e.g., Kerandi et al., 2018). Although this approach reduces the number of

1 calibrated parameters, it has less flexibility because changing one factor will change all the
2 parameters that use the same proportion.
3
4 For the calibration exercises we conduct here, the retention depth factor (RETDEPRTFAC) is
5 fixed at 0.001. This value is reasonable because the modeled discharge of our particular
6 configuration (Sec. 2.2) using default parameters is lower than observed discharge. Reducing this
7 factor from 1 to 0.001 keeps less water in water ponds and more water on the surface so it can
8 contribute to river discharge. First, we calibrate 48 parameters based on a 3-day simulation from
9 April 9 to April 11, 2013 (Table S1 in Supporting Information). This calibration uses the
10 estimation mode in the PEST tool and considers equal weight for all four USGS stations. We
11 calibrate Manning's roughness coefficients for both channels and land-use types, the deep drainage
12 (SLOPE), infiltration-scaling parameter (REFKDT), and saturated soil lateral conductivity
13 (REFDK). Manning's roughness coefficients control the hydrograph shape and the timing of the
14 peaks; the SLOPE, REFKDT, and REFDK control the total water volume. Second, based on the
15 knowledge we learn from the 48-parameter calibration (see details in Sec. 4.1), for the same 3-day
16 period, we reduce the number of calibrated parameters from 48 to 22 according to the sensitiveness
17 of the WRF-Hydro model to the adjustable parameters. For example, during the calibration we
18 find that Manning's roughness coefficients for several land types barely change because these land
19 types (e.g., tundra, snow/ice) are not present in the study area. We also learn that even though the
20 calibrated WRF-Hydro parameters can generate discharge results that closely resemble
21 observations, the physical meaning of several parameters are not appropriate because of the wide
22 range of those parameters that we set in the PEST control file. For example, Manning's roughness
23 coefficient for stream order 1 (0.199) is calibrated smaller than that for stream order 2 (0.218); the
24 overland roughness coefficients for evergreen needleleaf forest (0.043) and mixed forest (0.023)
25 are calibrated smaller than for cropland/woodland (0.046). Neither of these is true in the real world.
26 We therefore adjust the range of many parameters according to the literature (Soong et al., 2012)
27 to maintain their physical meanings (Table 1). We find that by using the same absolute weight for
28 all four stations, the calibration helps three stations (Station 2, 3, and 4) with large water volumes
29 to generate more reasonable results than do the default parameters; however, the results for Station
30 1, which has a relatively small volume of water, is not always better than the discharge that is
31 modeled by using default parameters. Thus, we assign a weight of 9.0 for Station 1 versus a weight

1 of 1.0 for the other three stations according to the inversed mean of observed discharge over these
2 four stations in April 2013. The ratio of the weights between Station 1 and the other three stations
3 stays similar even if the means are calculated based on different time periods.
4

5 **3.4 Statistics**

6 This study employs three statistical criteria: Nash–Sutcliffe efficiency (NSE; Nash and Sutcliffe,
7 1970; Moriasi et al., 2007), root-mean-square error (RMSE), and Pearson correlation coefficient
8 (PCC). RMSE and PCC evaluate model performance in terms of bias and temporal variation. NSE
9 quantitatively describes the accuracy of modeled discharge compared with the mean of the
10 observed data. Equation (1) calculates the NSE with defined variables:

$$11 \quad NSE = 1 - \frac{\sum_{t=0}^n (Y_t^{obs} - Y_t^{sim})^2}{\sum_{t=0}^n (Y_t^{obs} - Y_{mean}^{obs})^2}, \quad (1)$$

12 where Y_t^{obs} is the t th observed value from USGS sites for river discharge, Y_t^{sim} is the t th
13 simulated value from the WRF-Hydro output, Y_{mean}^{obs} is the temporal average of USGS observed
14 discharge, and n is the total number of observation time points. An efficiency of 1 ($NSE = 1$)
15 corresponds to a perfect match between modeled discharge and observed data. An efficiency of 0
16 ($NSE = 0$) indicates that the model predictions are as accurate as the mean of the observed data.
17 An efficiency below zero ($NSE < 0$) occurs when the model is worse than the observed mean.
18 Essentially, the closer the NSE is to 1, the more accurate the model is.

19 **4 Results**

20 **4.1 WRF-Hydro calibration and validation**

21 Based on the knowledge we gained from the 48-parameter 3-day calibration, we adjust the range
22 of critical parameters in the PEST control file to maintain their physical meanings. For example,
23 we set Manning’s roughness coefficient larger for stream order 1 than for stream order 2. We also
24 adjust the parameter range of the overland roughness coefficient for multiple land covers, such as
25 forests. We exclude the parameters that is not sensitive to WRF-Hydro streamflow for this study,
26 in order to constrain the problem size considering the availability of computational resources.
27 However, if the studied area is much larger with more land types than the study area here, then

1 there would be more parameters to calibrate. Hundreds of constant parameters in the Noah-MP
2 model could affect the WRF-Hydro results (Cuntz et al. 2016) and can be calibrated as well. Both
3 these situations would increase the burden of WRF-Hydro calibration. We perform the same 3-
4 day calibration from April 9 to April 11, 2013. Figure 2 shows the results of the 3-day modeled
5 discharge (in cubic meters) using default and calibrated parameters after five iterations, as well as
6 observed discharge. The four stations are calibrated by considering different weights. While the
7 model performance for Station 1 using default and calibrated parameters are similar, the calibration
8 improves the model performance over the drainage areas represented by Stations 2, 3, and 4
9 significantly. The modeled discharge using the default parameter underestimates the streamflow
10 by 24-33%. PEST detects this underestimation, immediately adjusts the parameters and increases
11 the modeled discharge during the first iteration. After the third iteration, the difference in calibrated
12 results between different iterations is relatively small. We allow the PEST to conduct five iterations
13 and use the parameters obtained from the fifth iteration as our optimum parameters. As shown in
14 Table 2, when the optimum parameters are used, the modeled discharges are much closer to the
15 observations than the modeled results using default parameters. The NSEs for the four stations
16 increased from -4.8 (Station 2), -18.8 (Station 3) and -57.0 (Station 4) to 0.75, -0.03, and -0.42,
17 respectively, being closer to 1. It is noteworthy that, threshold values to indicate a model of
18 sufficient quality have been suggested between $0.5 < \text{NSE} < 0.65$. Here, although we see the
19 calibration results close to the observations, the NSE are low for Stations 3 and 4. This may be
20 because the objective function used in PEST is sum of squared weighted residuals (SSWR), which
21 is calculated differently from NSE. Thus even if SSWR reaches a small value, the NSE might still
22 be far from 0.5 to 0.65. Incorporating other measures into the objective function of PEST may
23 improve the robustness of PEST calibrations. The RMSEs decreased from 902.2, 1001.3, and
24 $1399.3 \text{ m}^3/\text{sec}$ to 188.6, 228.7, and $219.1 \text{ m}^3/\text{sec}$, respectively.

25
26 During the validation period, compared with the modeled discharge using default parameters, as
27 shown in Table 2, the NSEs for all four stations are increased to be closer to 1; RMSEs are
28 significantly decreased; and the correlation coefficients between the observed and modeled
29 discharge are increased from 0.8, 0.7, 0.19, and 0.65 to 0.9, 0.81, 0.78, and 0.75. Compared with
30 the results of calibration using the estimation mode (no regularization) in PEST (not illustrated),
31 the SVD-based regularization generates slightly better hydrograph shape with 1-day later

1 discharge peaks that are closer to the observations. However, a problem remains with the
2 hydrograph shapes of the modeled discharge, especially with the modeled peak of discharge. For
3 Station 1, the WRF-Hydro almost captures the timing of the peak of discharge, but it still
4 underestimates the discharge by ~25%. One of the reasons perhaps is that this study uses a direct
5 pass-through baseflow module, which does not account for slow discharge and long-term storage
6 of the baseflow. Therefore, the largest contribution to river discharge is from precipitation, and
7 groundwater does not contribute much discharge to the channels in a long-term view, as is also
8 true for the other three large river stations. As a result, the contribution from the baseflow to the
9 river discharge in model simulations does not stay as long as in real situations. In the observations,
10 the river discharge decreases from the peak at a speed of ~500 m³/sec per day, while the modeled
11 river discharge decreases from the peak at a speed of ~1667 m³/sec per day. Using exponential
12 storage-discharge function for the baseflow may improve this situation. Other reasons include that
13 the parameter range we set in the PEST control file is perhaps not wide enough, as we can see
14 from Table 1 that, several optimal parameters hit the bound of parameter ranges. Allowing wider
15 parameter ranges may improve the calibration results.

16

17 Alternatively, instead of calibrating the stations that have large drainage area and water coming
18 from outside of the current model domain, we have also tested calibrating small flows at local
19 stations that have relatively small drainage area covered by the current study area. This requires to
20 generate a new high-resolution GIS data file to distribute the stations of interest. We first run the
21 WRF-Hydro model for 6 month using default parameters to spin up the model, and then we
22 calibrate the model based on observations of these local stations. Results including figures and
23 tables are shown in Supporting Information. The calibration results are improved compared to the
24 results that use default parameters, although further improvements are still needed. This again may
25 be because the parameter range are not wide enough to consider the possible values of parameters
26 that work for these specific areas represented at local stations, as we see many optimal parameters
27 hit the bound of the parameter range. More tests to figure out a better set of parameters are needed
28 for future investigation, which is beyond the scope of this study, since our goal is to present the
29 feasibility of HPC enabled PEST.

30

1 **4.2 Computational benefits of parallel PEST on HPCs**

2 The ability to scale up the calibration of WRF-Hydro by using parallel PEST on HPC systems is
3 determined by two factors: the scale-up capability of parallel PEST and the scale-up capability of
4 WRF-Hydro. In calibrating WRF-Hydro, PEST first makes as many model runs as there are
5 adjustable parameters to calculate Jacobian matrix (Doherty, 2016). The Jacobian matrix has a
6 column for each calibrated parameter and a row for each observation and each item of prior
7 information that set in the PEST control file. These model runs are independent between workers
8 and can be easily parallelized. Each worker runs the model with temporarily incremented
9 parameters that are defined in the template and control files. Then, PEST needs to make additional
10 model runs to test parameter updates. Different from the Jacobian runs, these additional runs are
11 performed by using different Marquardt lambdas, and the search for a Marquardt lambda that
12 achieves the best set of parameters is a serial iterative process. The lambda to use for the next run
13 depends on the outcome of the model run conducted using the previously chosen lambda. Although
14 serial testing of Marquardt lambdas may quickly find the optimal Marquardt lambda in the first or
15 second series of model runs, it is an inefficient use of computing resources because other
16 processors are idle while only one process is searching the lambdas. This is especially true when
17 the model domain is large and requires extensive computing resources. This study employs “partial
18 parallelization” for the lambda-testing procedure (Doherty, 2016), so multiple workers can be used
19 to calculate parameter upgrades based on a series of lambda values that are related to each other
20 by a factor of RLAMFAC set in the PEST control file. We also set the value of PARLAM to -9999
21 in the management file so only one cycle of parallel WRF-hydro runs is devoted to testing
22 Marquardt lambdas. For additional details on these parameters and their settings see the PEST
23 User Manual (Doherty, 2016).

24
25 In this study we test the computational performance of HPC-enabled parallel PEST using different
26 number of workers (6, 12, and 23) for the 22-parameter calibration. As shown in Table 3, we
27 conducted six experiments: Test 1 uses 23 workers, Test 2 uses 12 workers, and Test 3 uses 6
28 workers. All three tests use two nodes for each worker to run WRF-Hydro in parallel. The
29 maximum number of lambda-testing runs undertaken per iteration is set to 15, 10, and 5 for Tests
30 1, 2, and 3, respectively, to assure that only one cycle of WRF-hydro runs is devoted (using 15, 10
31 and 5 workers from Tests 1, 2, and 3, respectively) to testing Marquardt lambdas. Note that the

1 maximum number of lambda-testing runs should be set equal to or less than the workers available.
2 Otherwise, another cycle of WRF-hydro runs needs to be conducted. In fact, generating more
3 Marquardt lambdas does not always guarantee that the best Marquardt lambdas are generated. In
4 contrast, it may make the model convergence slower (here, PEST) or even model failure.

5
6 In order to test the trade-offs between the computing nodes used for running parallel WRF-Hydro
7 and the workers used for running parallel PEST, Tests 4, 5 and 6 use the same number of workers
8 (six) as Test 3 but use different number of nodes for each worker to run WRF-Hydro in parallel.
9 Explicitly, Test 4 uses four nodes per worker, Test 5 uses six nodes per worker, and Test 6 uses
10 eight nodes per worker. The maximum number of lambda-testing runs undertaken per iteration is
11 set to five for Tests 4, 5 and 6. Note that the time costs in Table 3 are limited to only one iteration.
12 Conducting more iterations will increase the cost of wall-clock time and computing resource, but
13 will not change the conclusion for the scale-up capability and computational benefits for HPC-
14 enabled parallel PEST linked to WRF-hydro.

15
16 PEST needs to run the WRF-Hydro model at least as many times as the number of calibrated
17 parameters (22 here). In fact, PEST runs the model 23 times in the first round (or the first iteration)
18 with initial parameter values and for the first Jacobian matrix. From the second iteration, it runs
19 the model 22 times to calculate Jacobian matrix. Therefore, if there are fewer than 23 workers, the
20 time cost for the first round of Jacobian matrix calculation will increase accordingly. For example,
21 as shown in Fig. 4a, when we assign 12 (and 6) workers to parallel PEST, the time cost for
22 calculating the Jacobian matrix is increased by a factor of 2 (and 4) compared with the time cost
23 of using 23 workers. The time cost for the parameter upgrade stays similar for the three
24 experiments because only one cycle of WRF-hydro simulation is conducted to test the Marquardt
25 lambdas. As a result, the total time cost for Test 2 is ~1.5 times more than that for Test 1, and the
26 total time cost for Test 3 is ~1.5 times more than that for Test 2 (Fig. 4b). By extrapolating the
27 speedup curve shown in Fig. 4a and Fig. 4b, we expect the total time cost to be ~1516 minutes
28 when using only one worker (or sequential mode), which is about 15 times slower compared with
29 running the PEST in parallel mode using 23 workers. For this particular study with 22 adjustable
30 parameters, we expect the time cost most likely to stay the same even if one increases the number
31 of workers to more than 23, because PEST runs WRF-Hydro only 23 or 22 times for each iteration.

1 Assigning more workers for this particular study would most likely render some workers idle and
2 is not an efficient use of computing resources. PEST may run WRF-Hydro more than 22 times
3 (e.g., 44 times) if higher-order finite differences are employed. In this case, assigning more
4 workers (e.g. 45 workers) may further speed up the calibration process. On the other hand, for the
5 same case study and using the same number of nodes for running parallel WRF-Hydro, we can
6 estimate the computing speedup by assuming an increase in the number of calibrated parameters
7 to 50. This would be the case, for example, to evaluate model sensitiveness to the physics in Noah-
8 MP or the spatial variabilities of certain parameters. We then expect to use 51 workers to calculate
9 the Jacobian matrix in only one cycle. This would then be 28–30 times faster than running PEST
10 using one worker (or in sequential mode). Similarly, if 100 parameters were used for the calibration
11 for the same case study, a factor of up to 60 speedup in the calibration process would be achieved
12 by running HPC-enabled parallel PEST.

13

14 In addition, by increasing the number of nodes for each worker to conduct WRF-Hydro (Tests 3,
15 4, 5, and 6), the time cost for the entire calibration process is significantly reduced (Figs. 4c and
16 4d). Specifically, the WRF-hydro scales up well when using four, six, and eight nodes compared
17 with using two nodes per worker for running the WRF-Hydro. Both the time spent on calculating
18 the Jacobian matrix and the time spent on testing the parameter upgrades are decreased by 49%
19 67%, and 77%, respectively, when using four, six, and eight nodes. Therefore, the total time spent
20 is also decreased when using more nodes for each worker (see Table 3). Moreover, if one has a
21 larger study area such as the entire contiguous United States, we expect the WRF-Hydro to have
22 an even better scale-up capability (e.g., on dozens of nodes) than this study.

23

24 While these numbers in Table 3 and Figure 4 are helpful to demonstrate the scale-up capability of
25 each component (PEST and WRF-Hydro), they do not answer questions such as, if one has certain
26 number of nodes, how many workers and how many nodes per worker should be used to achieve
27 the highest efficiency of the WRF-Hydro calibration using HPC-enabled PEST? On the other hand,
28 one may have unlimited computational resource, but would like to complete the calibration in a
29 short time period. We present scalability analysis below to answer these questions. First, we
30 generate more scenarios using different number of workers and nodes per worker by extrapolating
31 the existing time and computing costs based on the experiments that are already conducted. These

1 scenarios use 23 or 12 workers, and 4, 6, or 8 nodes per worker, respectively. Since we have
2 conducted simulations using the same number of nodes per worker, the cost for these scenarios are
3 easily predicted.

4
5 As shown in Figure 5, compare with Test 3 (which requires the least computing resource —12
6 nodes in total), having more workers (with the same number of nodes for each worker, e.g., Tests
7 1 and 2), takes more time than the ideal curve. The ideal curve assumes a linear speedup based on
8 the time cost of Test 3. However, using the same number of workers and increasing the number of
9 nodes for each worker (e.g., Tests 4, 5, and 6) can achieve the ideal speedup. Even when using 12
10 workers, increasing the number of nodes for each worker can still achieve a speedup close to the
11 ideal curve. Using 23 workers will not achieve the ideal speedup. Therefore, if one only has a
12 certain number of nodes available, we recommend to use relatively small number of workers but
13 large number of nodes for each worker. For example, if one has 48 nodes, then there are three
14 options can be considered: using 23 workers and 2 nodes per worker; 12 workers and 4 nodes per
15 worker, and 6 workers and 8 nodes per worker. Other partition (16x3; or 8x6) between numbers
16 of workers and nodes per worker are not as efficient as above. These three options will cost 103,
17 72 and 60 min, respectively, to finish one iteration. Thus, using 6 workers and 8 nodes per worker
18 is the most efficient way to consume the limited computing resource. On the other hand, if one
19 would like to conduct the calibration in a short time period without any limits for the computing
20 resource, then using 23 workers and 8 nodes (perhaps even more nodes depending on the size of
21 the model domain and the scale up capability of WRF-Hydro), will finish one iteration in ~24 min.
22

23 **4.3 Evaluation of spatial transferability of the calibrated parameters**

24 To assess the transferability of the calibrated parameters, we apply the optimum parameters
25 obtained from the calibration for the four stations (black circles) in Fig. 1 to another set of four
26 stations (crosses in Fig. 1) in the study area. All four sites are located on relatively small rivers, so
27 the lag time between precipitation peak and the discharge peak are much shorter than that for the
28 stations on the lower part of MRB (e.g., Stations 2, 3, and 4). The assessment compares the
29 observed discharge with the closest grid cells from the discharge output of WRF-Hydro. Figure 6
30 shows the observed and modeled discharge using default and the optimum parameters. Overall,

1 WRF-Hydro's default parameters underestimate the discharge and misrepresent the timing of
2 discharge peaks compared with observations over the four assessed stations (Stations 5, 6, 7, and
3 8). By using the calibrated parameters from other sites over the area, the model results increase the
4 discharge and shift the hydrograph shape so they are much closer to the observations than model
5 results using default parameters. The absolute error of simulated discharge decreases by 13.1%,
6 38.3%, and 71.6%, respectively, over Stations 6 through 8 (Station 5 shows a 6% increase of
7 absolute error), compared with the default simulated discharge. We also find that using the SVD-
8 based regularization for the PEST calibration captures the timing of discharge peak better than
9 using the estimation mode, which is one-day earlier than the observations reaching the discharge
10 peak.

11 **5 Summary and discussion**

12 WRF-Hydro is a new, and perhaps the first practical, computer code that can run on HPC systems
13 and can model the entire hydrological cycle using physics-based submodels and high-resolution
14 input datasets (e.g., radar). The hydrological community has desired this capability for decades,
15 although it requires intensive computing resources. Thus, the calibration of this model would
16 ideally be conducted on HPCs in parallel as well, especially when the model covers a large domain
17 rather than the basin scale. This study ports an independent model calibration tool, parallel PEST,
18 to HPC clusters and links it to WRF-Hydro to help WRF-Hydro users calibrate the model within
19 a much shorter wall-clock time period. The bridge we build here (between parallel PEST and
20 WRF-Hydro on the basis of HPC systems) can be applied to any other hydrological models and
21 Earth system models that use parameterizations to represent model physics. We present the
22 operational feasibility of the HPC-enabled parallel PEST by evaluating the performance of
23 calibrated WRF-Hydro against observation in hydrograph features such as volume and timing of
24 flood events. We examine the scale-up capability and computational benefits of the tool by
25 assigning different computing resource for PEST and for WRF-Hydro. While this study presents
26 the optimum parameters identified from the calibration of the particular flood event, the parameters
27 can be significantly different if one uses different physics, such as exponential storage-discharge
28 function for a groundwater model or reach-based channel routing. Our preliminary testing shows
29 that using exponential storage-discharge function with the default parameters provided by WRF-
30 Hydro, the modeled discharge was larger than that of observations. Thus, the calibration will need

1 to adjust the parameters to reduce the discharge. Our study finds that for calibrating 22 parameters,
2 using the same computing resource for running WRF-hydro, the HPC-enabled PEST calibration
3 tool can speed up WRF-Hydro calibration by a factor of 15, compared with running PEST in
4 sequential mode. The speedup factor can be larger when the number of parameters needing
5 calibration is higher (e.g., 50 or 100).

6
7 The following are several key points that we would like to mention to inform future studies:

- 8 1. In this study, we consider using the prior or regularization information only for the
9 parameters that we calibrate. As is the case with solving inverse problems, prior
10 information is added to improve the smoothness of the solutions. In order to build a more
11 comprehensive calibration, an important aspect that can be considered is to enrich the prior
12 with the available historical data. For example, in this particular case, one can use the
13 historical observation data (e.g., April and May from the past few years) to enrich the prior
14 information for the parameters. Hence, the regularization objective function in PEST will
15 constitute not only the discrepancies between parameters and their “current estimates” but
16 also the discrepancies between WRF-Hydro simulations and preferred values (which is the
17 observed time series of historical discharge). Additionally, one can use the pilot points
18 technique described by Doherty (2005) in conjunction with parameter estimation to add
19 more flexibility to the calibration process. This will be potentially beneficial in improving
20 the predictions.
- 21 2. To focus on our main goal, we calibrate only the parameters in lookup tables. However,
22 we acknowledge that using a single value to represent a physics for a large domain could
23 be problematic, especially we expect the HPC-enabled parallel PEST to execute with
24 WRF-Hydro for large domains. This situation often needs parameter regionalization. For
25 example, WRF-Hydro version 5.0 has many spatially distributed parameters available,
26 such as OVROUGHRTFAC— the overland flow roughness scaling factor,
27 RETDEPRTFAC— the factor of maximum retention depth, and the soil-related parameters
28 (when compiled with SPATIAL_SOIL=1). Calibrating these spatial parameters based on
29 grid scale (e.g., catchments) rather than a single value will give the model more flexibility
30 and thus better fit the observations (Hundecha and Bardossy, 2004; Wagener and Wheater,
31 2006). In practice, for example, one can include regional OVROUGHRTFACs (e.g., their

1 lower/upper bounds, and default values) in the PEST control file based on catchments.
2 However, the selection of the locations and sizes of catchment may introduce significant
3 uncertainties to the calibration results, which require systematic and comprehensive
4 investigation and understanding of the study area.

- 5 3. This study is limited to calibrating the observed streamflow only based on the format of
6 one of WRF-Hydro model outputs for individual station or point (frxst_pts_out.txt). It is
7 feasible, however, to calibrate other variables as long as the observation data is available.
8 For example, one can either find the closest point from the gridded dataset to the
9 observation location and then compare that model grid to observations; or one can change
10 the WRF-Hydro input/output code to output other variables in the frxst_pts_out.txt file, so
11 they can still use the same interface we developed here to calibrate other variables in
12 addition to the discharge.
- 13 4. The optimal parameter set obtained from this study is from the 5th iteration of parallel
14 PEST by testing five Marquardt lambdas. Testing different number of lambdas or
15 calibrating different number of parameters may generate a different set of optimal
16 parameters. These parameter sets can all make physical sense and be equally good for
17 reproducing observed discharges. This problem is named equifinality (Beven and Freer,
18 2001; Savenije, 2001), which is an important source of model uncertainty. To reduce the
19 model uncertainty through reducing the equifinality, hydrologists carry out additional
20 modelling objective for model evaluation to find more useful parameter sets (Mo and
21 Beven, 2004; Gallart et al., 2007). Alternatively, inspired by No. 3 discussed above, one
22 can calibrate the WRF-hydro model based on more than one variables, such as discharge
23 and soil moisture (or heat flux or water table depth) to reduce the number of optimal
24 parameter sets, and thus reduce the model uncertainty of predictions for these variables.
- 25 5. While this study ported the parallel PEST to HPC system and linked it to WRF-Hydro, we
26 note that BEOPEST is available in the PEST family. BEOPEST has the same functionality
27 as parallel PEST but uses a different approach for communication between master and
28 workers. Working with HPC-enabled BEOPEST may save total time cost since BEOPEST
29 uses the Transmission Control Protocol and the Internet Protocol instead of message files
30 (reading input and writing output between master and works) for communication. We
31 expect it to be relatively straightforward to use BEOPEST to calibrate WRF-hydro on

1 HPCs since the interface remains the same, except one needs to copy the template and
2 instruction files in addition to the global files (see Section 3.1) into each working folder.

3
4 *Data and Code availability.* The observed river discharge is downloaded from the USGS Surface-
5 Water Data website, available at <https://waterdata.usgs.gov/nwis/sw>. The Stage IV precipitation
6 data were downloaded from <https://data.eol.ucar.edu/dataset/21.093>. PEST was downloaded from
7 <http://www.pesthomepage.org/Downloads.php>. We use the Unix PEST version 13.6. The scripts
8 and files that are developed in this study and required by PEST for calibrating WRF-Hydro are
9 available at <http://doi.org/10.5281/zenodo.3247116>.

10
11 *Author contributions.* JW proposed the project and developed the study case in WRF and WRF-
12 Hydro. CW developed the scripts/code to port the parallel PEST to DOE supercomputers and adapt
13 it to work with WRF-Hydro. VR provided important input for the regularization calibration
14 method. AO operated the ArcGIS tool to delineate the high-resolution grid cells to include stream
15 channel network, open water, and groundwater/baseflow basins. EY provided important input for
16 hydrology during the revision of this manuscript. RK provided high-level guidance and insight for
17 the entire project. All authors commented on this manuscript.

18
19 *Competing interests.* The authors declare that they have no conflict of interest

20
21 *Acknowledgments.* This work is supported under a Laboratory Directed Research and
22 Development (LDRD) Program at Argonne National Laboratory, through U.S. Department of
23 Energy (DOE) contract DE-AC02-06CH11357. Computational resources are provided by the
24 DOE-supported National Energy Research Scientific Computing Center, Argonne National
25 Laboratory Computing Resource Center, and Argonne Leadership Computing Facility. Our special
26 thanks to the PEST developers and entire WRF-Hydro team, especially Kevin Sampson for his
27 guidance on the ArcGIS tool. We gratefully thank the two reviewers for their valuable comments
28 and suggestions, which tremendously improved this manuscript.

1 **References**

2 Arnault, J., Wagner, S., Rumlmer, T., Fersch, B., Bliefernicht, J., Andresen, S., and Kunstmann,
3 H.: Role of runoff–infiltration partitioning and resolved overland flow on land–atmosphere
4 feedbacks: A case study with the WRF-Hydro coupled modeling system for West Africa, *J.*
5 *Hydrometeorol.*, 17, 1489–1516, 2016.

6
7 Beven, K., and Freer, J.: Equifinality, data assimilation, and uncertainty estimation in mechanistic
8 modelling of complex environmental systems using the GLUE methodology, *J. Hydrol.*, 249, 11-
9 29, 2001.

10
11 Campos, E., and Wang, J.: Numerical simulation and analysis of the April 2013 Chicago Floods,
12 *J. Hydrol.*, 531, 454–474, 2015.

13
14 Chen, F. and Dudhia, J.: Coupling an advanced land surface-hydrology model with the Penn State-
15 NCAR MM5 modeling system, Part I: Model implementation and sensitivity, *Mon. Weather Rev.*,
16 129, 569–585, 2001.

17
18 Cuntz, M., Mai, J., Samaniego, L., Clark, M., Wulfmeyer, V., Branch, O., Attinger, S., and Thober,
19 S.: The impact of standard and hard-coded parameters on the hydrologic fluxes in the Noah-MP
20 land surface model, *J. Geophys. Res. Atmos.*, 121, 10,676–10,700, doi:10.1002/2016JD025097,
21 2016.

22
23 Doherty, J.: PEST: Model Independent Parameter Estimation, User Manual, 6th ed., Watermark
24 Numerical Computing, Brisbane, Queensland, Australia, 2016.

25
26 Doherty, J.: Ground water model calibration using pilot points and regularization, *Groundwater*,
27 41(2), 170–177, 2005.

28
29 Gallart, F., Latron, J., Llorens, P., and Beven, K. J.: Using internal catchment information to reduce
30 the uncertainty of discharge and baseflow predictions. *Adv. Water Resour.* 30(4), 808–823, 2007.

31

1 Getirana, A. C. V.: Integrating spatial altimetry data into the automatic calibration of hydrological
2 models, *J. Hydrol.*, 387 (3-4), 244–255, doi: 10.1016/j.jhydrol.2010.04.013, 2010.
3
4 Gochis, D. J., Barlage, M., Dugger, A., FitzGerald, K., Karsten, L., McAllister, M., McCreight, J.,
5 Mills, J., RafieeiNasab, A., Read, L., Sampson, K., Yates, D., and Yu, W.: The WRF-Hydro
6 modeling system technical description, (Version 5.0). NCAR Technical Note. 107 pages.
7 Available online at:
8 <https://ral.ucar.edu/sites/default/files/public/WRFHydroV5TechnicalDescription.pdf>, 2018.
9
10 Hundecha, Y., and Bárdossy, A.: Modeling of the effect of land use changes on the runoff
11 generation of a river basin through parameter regionalization of a watershed model, *J. Hydrol.*,
12 292, 281–295, 2004.
13
14 Kerandi, N., Arnault, J., Laux, P., Wagner, S., Kitheka, J., and Kunstmann, H.: Joint atmospheric-
15 terrestrial water balances for East Africa: A WRF-Hydro case study for the upper Tana River basin,
16 *Theor. Appl. Climatol.*, 131, 1337–1355, doi: 10.1007/s00704-017-2050-8, 2018.
17
18 Lin, Y., and Mitchell, K. E.: The NCEP stage II/IV hourly precipitation analyses: Development
19 and applications, Preprints, 19th Conf. on Hydrology, San Diego, CA, Amer. Meteor. Soc., 1.2.,
20 2005.
21
22 Madsen, H.: Automatic calibration of a conceptual rainfall–runoff model using multiple
23 objectives, *J. Hydrol.*, 235, 276–288, 2000.
24
25 Mo, X., and Beven, K.: Multi-objective parameter conditioning of a three-source wheat canopy
26 model. *Agricultural & Forest Meteorol.* 122(1–2), 39–63, 2004.
27
28 Moriasi, D. N., Arnold, J. G., Van Liew, M. W., Bingner, R. L., Harmel, R. D., and Veith, T. L.:
29 Model evaluation guidelines for systematic quantification of accuracy in watershed simulations,
30 *Transactions of the ASABE*, 50 (3), 885–900, 2007.
31

1 Nash, J. E., and Sutcliffe, J. V.: River flow forecasting through conceptual models, part I – A
2 discussion of principles, *J. Hydrol.*, 10(3), 282–290, doi: 10.1016/0022-1694(70)90255-6, 1970.
3

4 Niu, G.-Y., Yang, Z.-L., Mitchell, K. E., Chen, F., Ek, M. B., Barlage, M., Kumar, A., Manning,
5 K., Niyogi, D., Rosero, E., Tewari, M., and Xia, Y.: The community Noah land surface model with
6 multiparameterization options (Noah-MP): 1. Model description and evaluation with local-scale
7 measurements, *J. Geophys. Res.*, 116, D12109, doi: 10.1029/2010JD015139, 2011.
8

9 NWS (National Weather Service): Record river flooding of April 2013,
10 <https://www.weather.gov/ilx/apr2013flooding>, 2013.
11

12 Prat, O. P., and Nelson, B. R.: Evaluation of precipitation estimates over CONUS derived from
13 satellite, radar, and rain gauge data sets at daily to annual scales (2002-2012), *Hydrol. Earth Syst.*
14 *Sci.*, 19, 2037–2056, doi: 10.5194/hess-19-2037-2015, 2015.
15

16 Sampson, K., and Gochis, D.: WRF Hydro GIS Pre-processing tools, Version 5.0 Documentation,
17 2018.
18

19 Sapiano, M. R. P., and Arkin, P.A.: An intercomparison and validation of high-resolution satellite
20 precipitation estimates with 3-hourly gauge data, *J. Hydrometeor.*, 10, 149–166, doi:
21 10.1175/2008JHM1052.1, 2009.
22

23 Senatore, A., Mendicino, G., Gochis, D. J., Yu, W., Yates, D. N., and Kunstmann, H.: Fully
24 coupled atmosphere-hydrology simulations for the central Mediterranean: Impact of enhanced
25 hydrological parameterization for short and long time scales, *J. Adv. Model. Earth Syst.*, 7(4),
26 1693–1715, doi: 10.1002/2015MS000510, 2015.
27

28 Savenije, H. H. G.: Equifinality, a blessing in disguise?, *Hydrol. Process.*, 15, 2835-2838, 2001.
29

30 Soong, D. T., Prater, C. D., Halfar, T. M., and Wobig, L. A.: Manning’s roughness coefficients for
31 Illinois streams, U.S. Geological Survey Data Series 668, 2012.

1
2 Tonkin, M. J., and Doherty, J.: A hybrid regularized inversion methodology for highly
3 parameterized environmental models, *Water Resource Research*, 41, W10412,
4 doi:10.1029/2005WR003995, 2005.
5
6 Wagener, T., and Wheater, H. S.: Parameter estimation and regionalization for continuous rainfall-
7 runoff models including uncertainty, *J. Hydrol.*, 320, 132–154, 2006.
8
9 Xia, Y., Mitchell, K., Ek, M., Sheffield, J., Cosgrove, B., Wood, E., Luo, L., Alonge, C., Wei, H.,
10 Meng, J., Livneh, B., Lettenmaier, D., Koren, V., Duan, Q., Mo, K., Fan, Y., and Mocko, D.:
11 Continental-scale water and energy flux analysis and validation for the North American Land Data
12 Assimilation System project phase 2 (NLDAS-2), 1: Intercomparison and application of model
13 products, *J. Geophys. Res.*, 117, D03109, doi: 10.1029/2011JD016048, 2012a.
14
15 Xia, Y., Mitchell, K., Ek, M., Cosgrove, B., Sheffield, J., Luo, L., Alonge, C., Wei, H., Meng, J.,
16 Livneh, B., Duan, Q., and Lohmann, D.: Continental-scale water and energy flux analysis and
17 validation for the North American Land Data Assimilation System project phase 2 (NLDAS-2). 2.
18 Validation of model-simulated streamflow, *J. Geophys. Res.*, 117, D03110, doi:
19 10.1029/2011JD016051, 2012b.
20
21 Yucel, I., Onen, A. Yilmaz, K. K., and Gochis, D. J.: Calibration and evaluation of a flood
22 forecasting system: Utility of numerical weather prediction model, data assimilation and satellite-
23 based rainfall, *J. Hydrol.*, 523, 49–66, 2015.

1 **Table 1: Calibrated 22 parameters and the optimum parameters found after five iterations,**
 2 **based on four USGS stations, indicated by the solid circle in Figure 1.**

Calibrated Parameter	Default	Lower Bound	Upper Bound	Optimum Parameter
mannn1	0.55	0.35	0.6	0.6
mannn2	0.35	0.15	0.35	0.35
mannn3	0.15	0.08	0.15	0.15
mannn4	0.1	0.05	0.15	5.00E-02
mannn5	7.00E-02	0.02	0.1	6.59E-02
mannn6	5.00E-02	0.015	0.1	4.67E-02
mannn7	4.00E-02	0.01	0.08	2.24E-02
mannn8	3.00E-02	0.005	0.06	1.72E-02
xslope1	0.1	1.00E-04	1	0.181358
refdk	2.00E-06	1.00E-08	1.00E-05	6.69E-07
refkdt	1	0.01	5	0.956414
ovn1 (urban)	2.50E-02	0.005	0.06	6.00E-02
ovn2 (dry crop)	3.50E-02	0.015	0.06	1.50E-02
ovn3 (irrigated crop)	3.50E-02	0.015	0.06	6.00E-02
ovn5 (crop/grass)	3.50E-02	0.015	0.06	1.50E-02
ovn6 (crop/wood)	6.80E-02	0.035	0.25	3.68E-02
ovn7 (grass)	5.50E-02	0.015	0.25	0.127159
ovn10 (savanna)	5.50E-02	0.015	0.3	0.157904
ovn11 (deciduous forest)	0.2	0.1	0.3	0.1
ovn14 (evergreen forest)	0.2	0.1	0.3	0.11768
ovn15 (mixed forest)	0.2	0.1	0.3	0.1
ovn16 (water)	5.00E-03	0.001	0.01	1.00E-02

1 **Table 2: Statistics of model performance using optimum and default (in parentheses)**
 2 **parameters for Stations 1–4 during the calibration and validation period.^a**

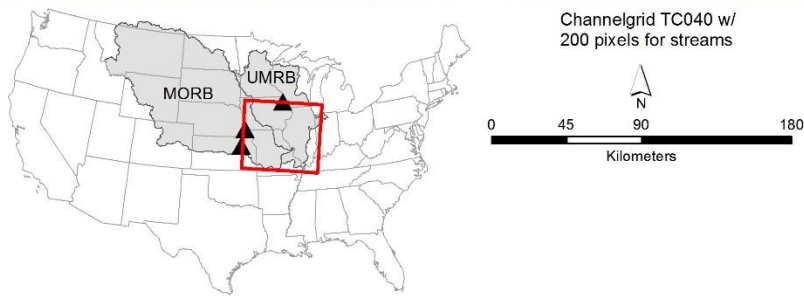
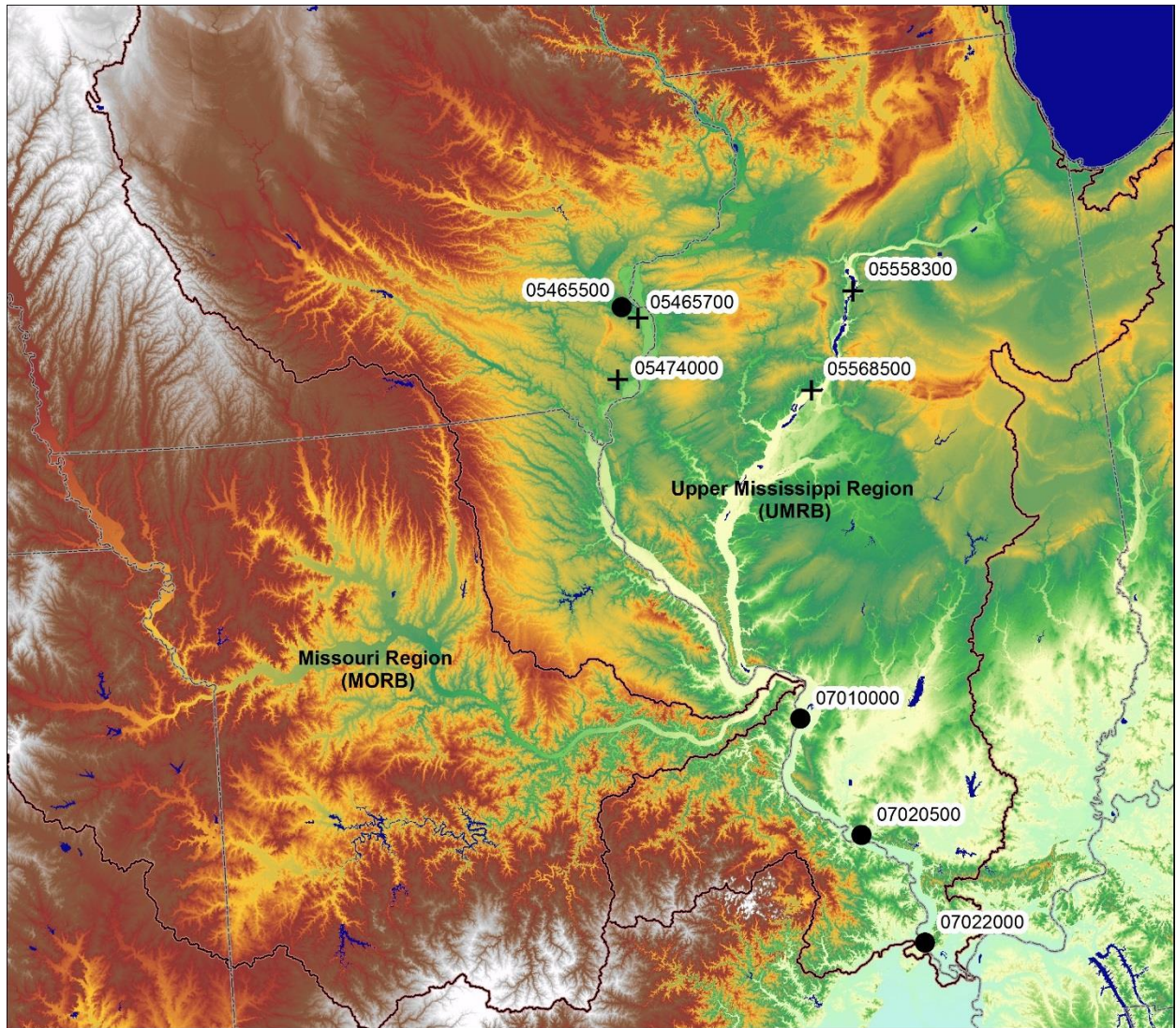
Statistics	Station 1	Station 2	Station 3	Station 4
Calibration				
NSE	0.64 (0.73)	0.75 (-4.8)	-0.03 (-18.8)	-0.42 (-57.0)
RMSE	79.8 (69.3)	188.6 (902.2)	228.7 (1001.3)	219.1 (1399.3)
PCC	0.92 (0.91)	0.91 (0.81)	0.86 (0.40)	0.50 (-0.52)
Validation				
NSE	0.52 (0.41)	0.17 (-0.62)	0.19 (-23.1)	0.09 (-0.76)
RMSE	440.6 (487.3)	2953.6 (4129.5)	2827.6 (15459.1)	3222.6 (4480.4)
PCC	0.9 (0.8)	0.81 (0.70)	0.78 (0.19)	0.75 (0.65)

3 ^a The calibration period is 3 days (April 9–11) and includes 22 parameters. The validation period
 4 is April 12–24. Bold typeface indicates the calibrated model results are closer to observations
 5 compared with the default model results. NSE and PCC are unitless; RMSE is in m³/sec.

- 1 **Table 3. Experiments designed to test the scale-up capability and computational benefits of**
- 2 **HPC-enabled parallel PEST linked to WRF-Hydro.**

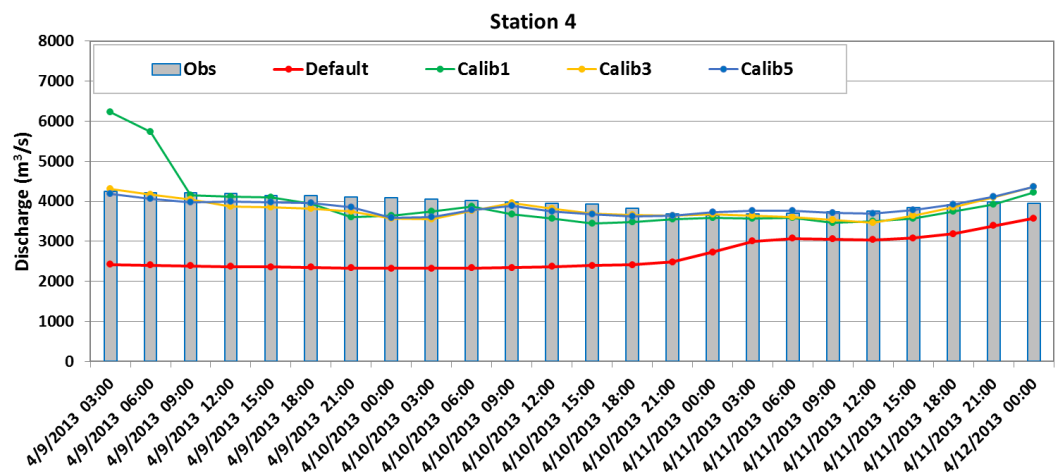
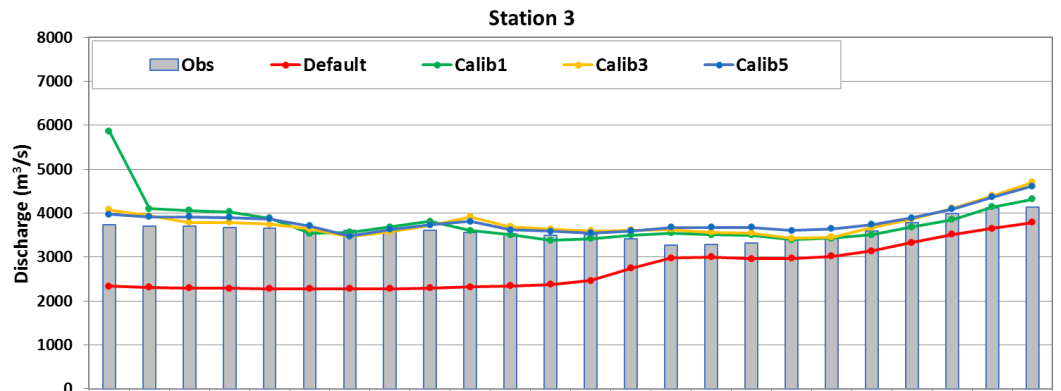
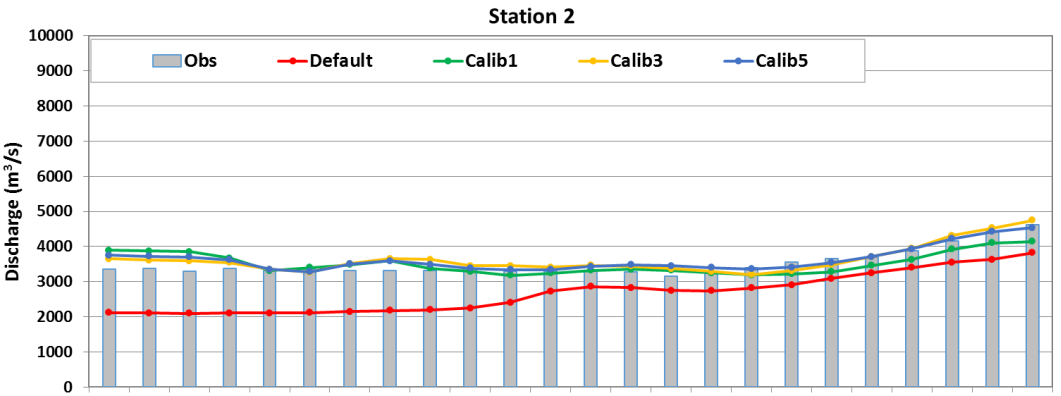
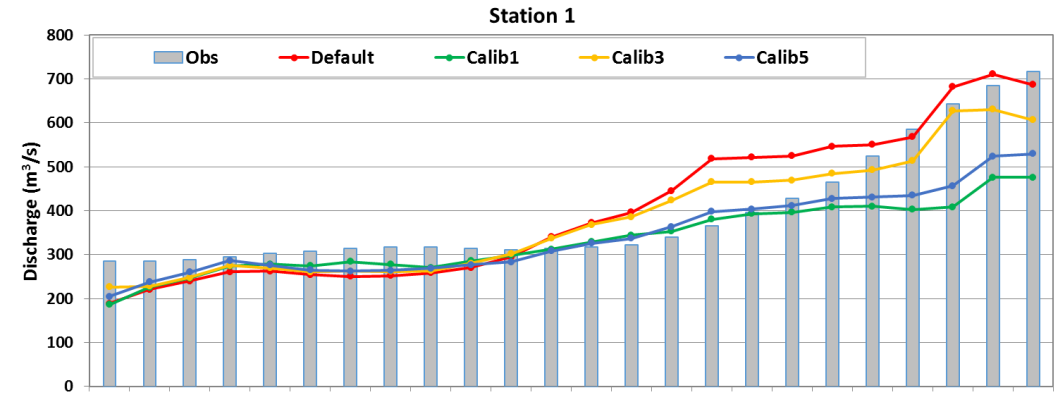
Test	No. of Workers	No. of Lamdas	No. of Nodes for Each Worker	Total computing resource (nodes)	Total Time Cost (min)	Time Cost for Calculating Jacobian Matrix	Time Cost for Testing Parameter Upgrades
Test 1	23	15	2	46	103	52	51
Test 2	12	10	2	24	150	102	48
Test 3	6	5	2	12	264	211	53
Test 4	6	5	4	24	131	107	24
Test 5	6	5	6	36	86	70	16
Test 6	6	5	8	48	60	48	12
Extrap. 1	23	15	4	92	48	24	24
Extrap. 2	23	15	6	138	32	16	16
Extrap. 3	23	15	8	184	24	12	12
Extrap. 4	12	10	4	48	72	48	24
Extrap. 5	12	10	6	72	48	32	16
Extrap. 6	12	10	8	96	36	24	12

3

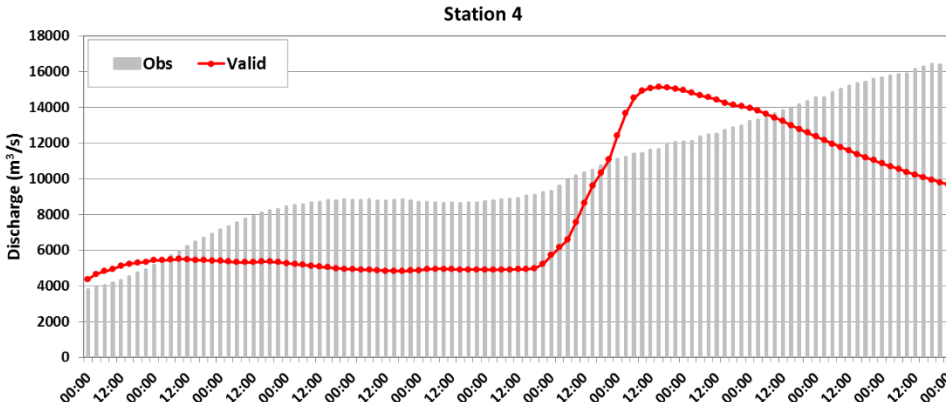
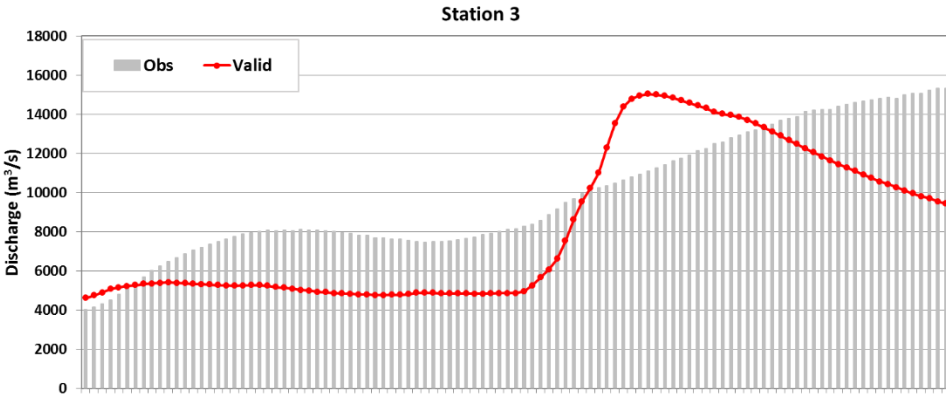
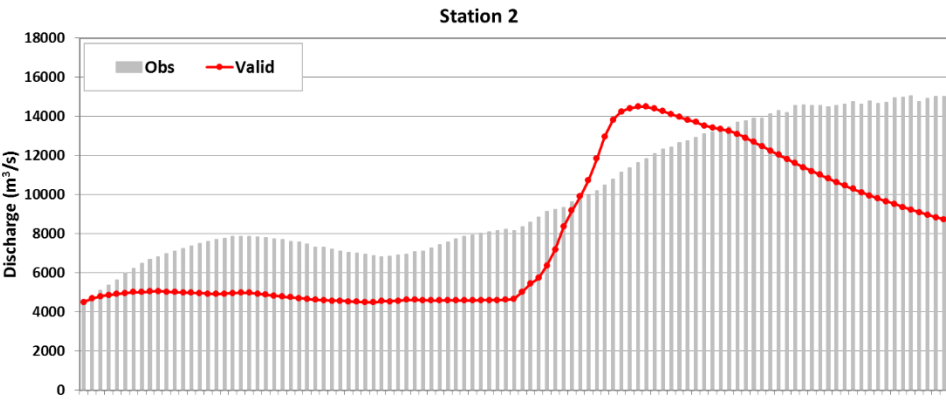
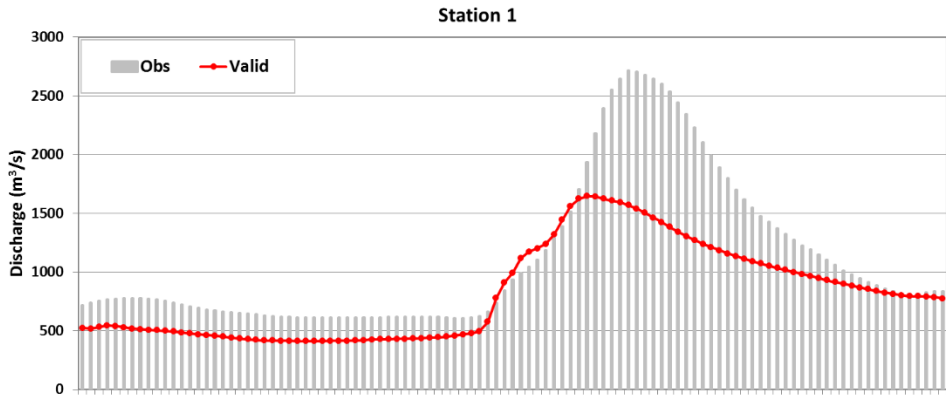


1
 2 **Figure 1: Eight USGS sites over the study area. The four circles are sites that are used for**
 3 **calibrations; the four crosses are sites that are used for transferability assessment. USGS site**
 4 **numbers corresponding to the site index used in this study are: Station 1: 05465500; Station**
 5 **2: 07010000; Station 3: 07020500; Station 4: 07022000; Station 5: 05465700; Station 6:**
 6 **05474000; Station 7: 05558300; Station 8: 05568500. The three inflow stations indicated by**

- 1 the black solid triangles are 06807000, 06887500, and 05389500. The boulder of Upper
- 2 Mississippi River Basin (UMRB) and Missouri River Basin (MORB) are highlighted.

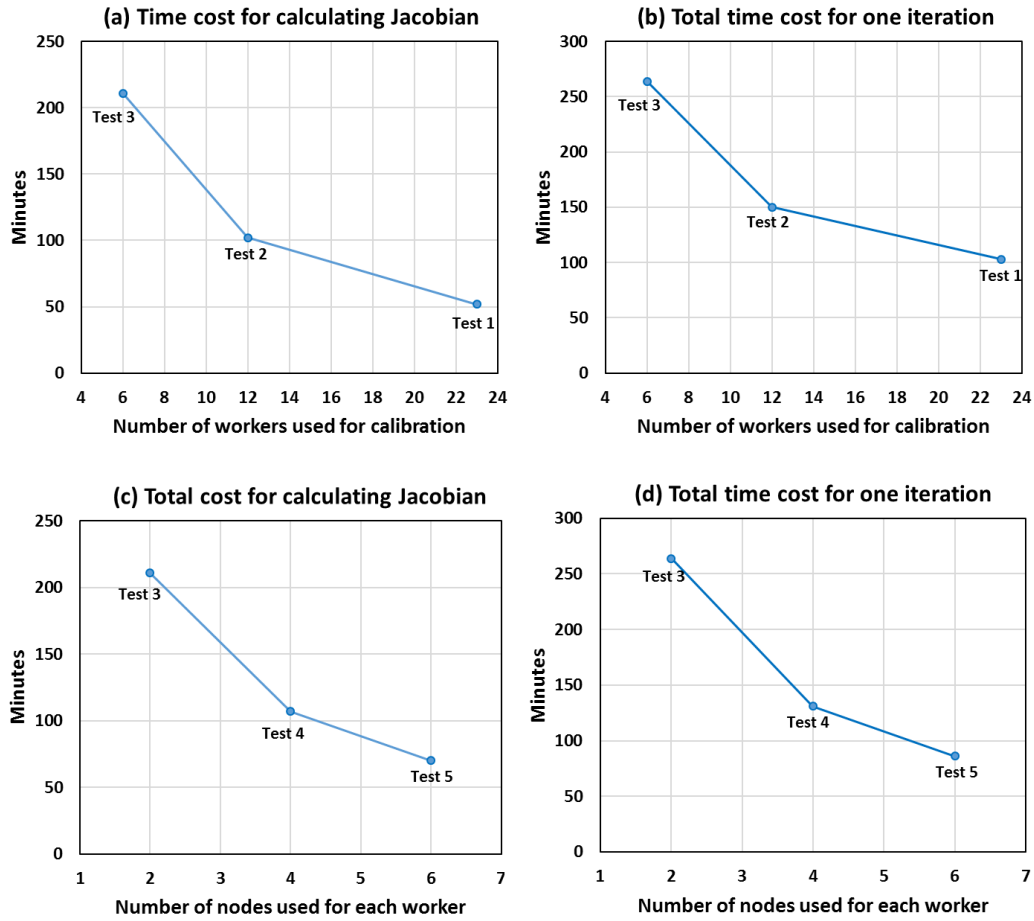


1 **Figure 2: Observed and modeled discharge (m^3/sec) using default and calibrated parameters**
2 **during a 3-day calibration period (April 9–11, 2013) over the four stations indicated by the**
3 **black circles in Fig. 1. The observed discharge for Stations 2, 3 and 4 are adjusted to exclude**
4 **the inflows from catchments that are not covered by current study area.**

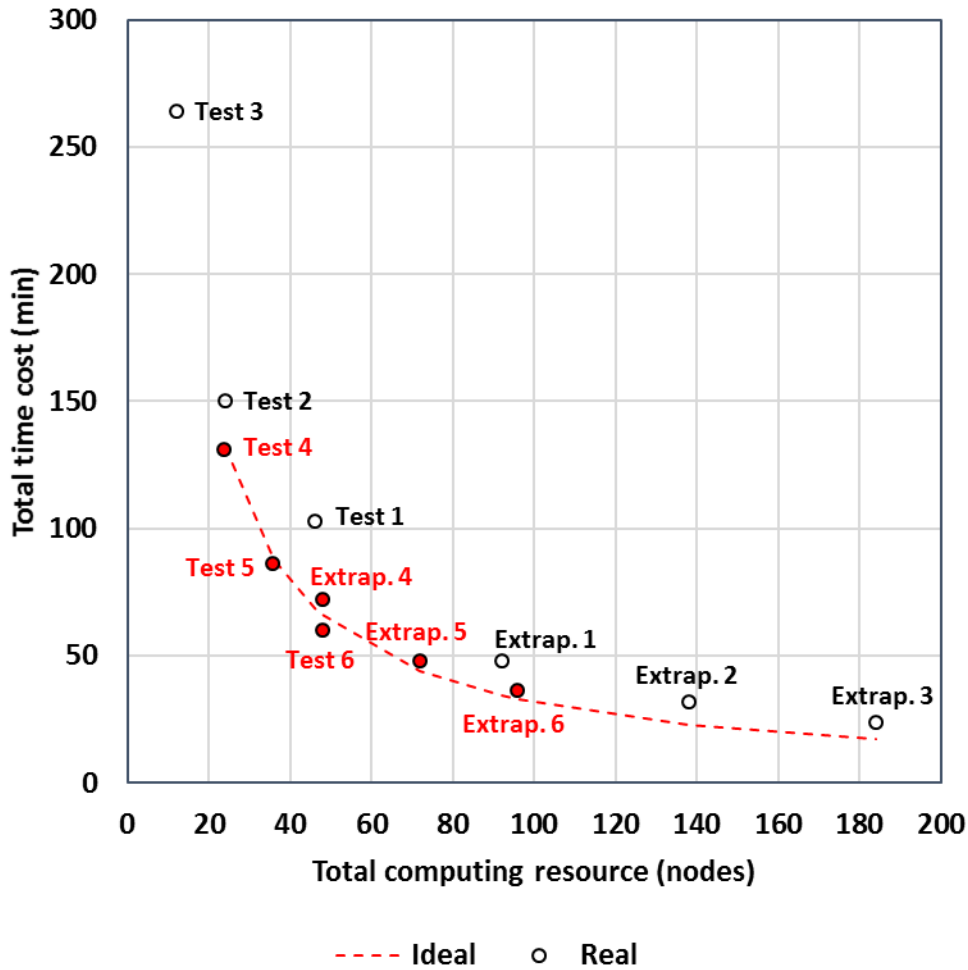


4/12/2013 00:00
 4/12/2013 12:00
 4/13/2013 00:00
 4/13/2013 12:00
 4/14/2013 00:00
 4/14/2013 12:00
 4/15/2013 00:00
 4/15/2013 12:00
 4/16/2013 00:00
 4/16/2013 12:00
 4/17/2013 00:00
 4/17/2013 12:00
 4/18/2013 00:00
 4/18/2013 12:00
 4/19/2013 00:00
 4/19/2013 12:00
 4/20/2013 00:00
 4/20/2013 12:00
 4/21/2013 00:00
 4/21/2013 12:00
 4/22/2013 00:00
 4/22/2013 12:00
 4/23/2013 00:00
 4/23/2013 12:00
 4/24/2013 00:00
 4/24/2013 12:00
 4/25/2013 00:00

1 **Figure 3: Observed and modeled discharge (m^3/sec) during a validation period (April 12–24,**
2 **2013) using optimum parameters identified from a 3-day calibration over the four stations**
3 **indicated by black circles in Fig. 1. Same as Figure 2, the observed discharge for Stations 2,**
4 **3, and 4 are adjusted.**

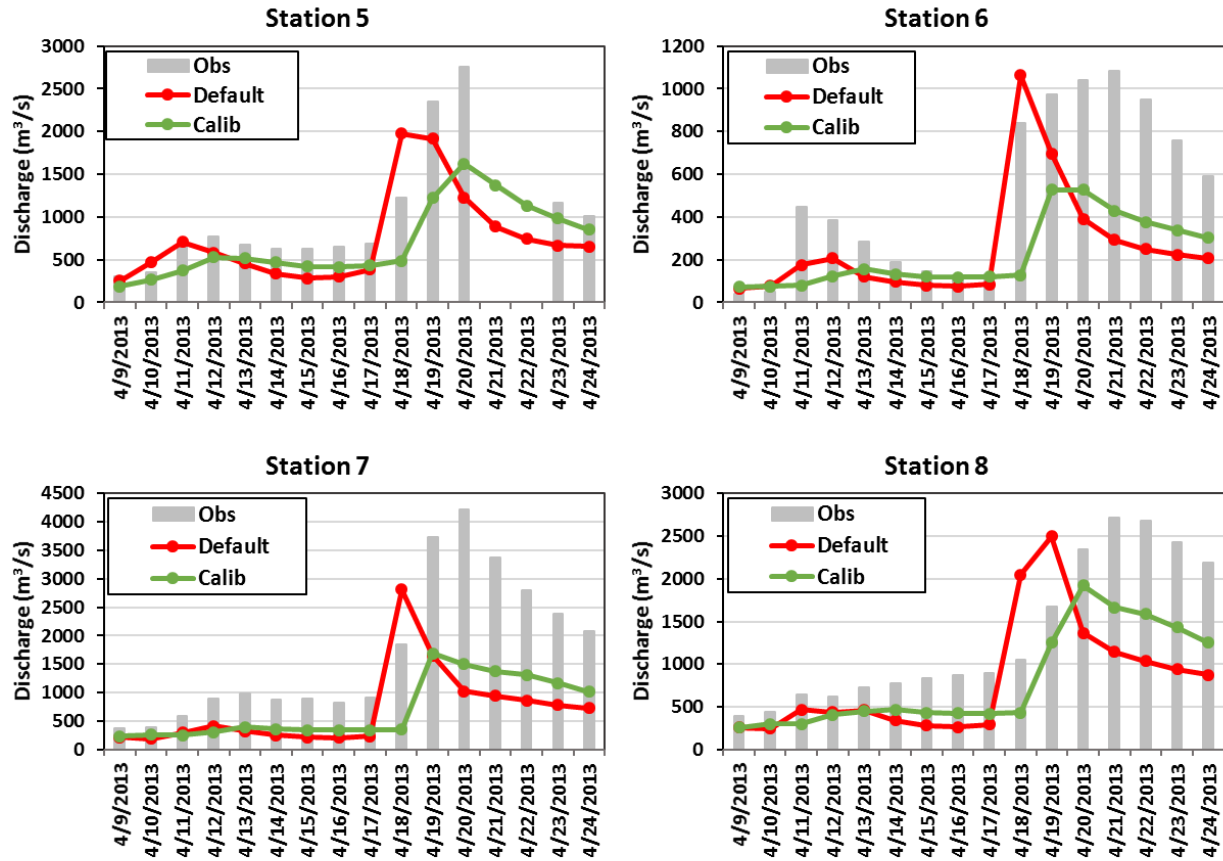


1
 2 **Figure 4. Time cost for calculating Jacobian matrix and total time cost for one iteration for**
 3 **five experiments (Table 3) using different number of workers to conduct PEST (a, b) and**
 4 **different number of nodes for each worker (c, d) to conduct WRF-Hydro.**



1
2
3
4
5
6
7
8

Figure 5. Total time cost and total computing resource needed for each test and extrapolated scenario, which uses different number of workers and different number of nodes per worker. The dash line is an ideal curve, which assumes a liner decrease in terms of time cost when more computing resource is used, built on Test 3. The circles are real cost for time and computing resource by each test and extrapolated. The red text and solid circles indicate those specific tests meet the ideal expectation of speedup.



1
 2 **Figure 6: Observed and modeled daily averaged discharge (m^3/sec) from April 9–24 using**
 3 **default and the optimum parameters (shown in Table 1) identified by the 3-day calibration**
 4 **over four stations that are in the study area (indicated by crosses in Fig. 1).**